

Frequency Reconfigurable Antenna with Dual-Band and Dual-Mode Operation

Ting-Yan Liu, Jun-Yan Chen, and Jeen-Sheen Row*

Abstract—A frequency reconfigurable antenna with dual-band operation is presented. The antenna has a circular radiating patch loaded with an annular slot, and the slotted patch is shorted to the ground plane with four conducting posts. The antenna has three feed ports. Two of the ports are used to excite the slot mode resonant at a lower frequency, and broadside radiation with dual orthogonal linear polarizations can be obtained. The other port is used to excite the monopolar-patch mode resonant at a higher frequency, and conical radiation with vertical polarization can be yielded. To reconfigure the operation frequencies, four varactors are symmetrically placed across the annular slot. The simulated results indicate that the resonant frequency of the slot mode can be tuned from 1.62 to 1.17 GHz when the capacitance of the varactors is varied from 0.6 to 1.8 pF; besides, for each capacitance value, the impedance bandwidth of the antenna operating in the monopolar-patch mode can cover the frequencies from 2.4 to 2.5 GHz. Experiments are also carried out to validate the simulated data.

1. INTRODUCTION

To cover the spectrums of different communication systems and relax the requirements of filters, frequency reconfigurable antennas with dual-band operation have received a great deal of attention, and several articles have been devoted to the antenna design [1–11]. The design in [1] uses a stacked patch antenna to realize dual-frequency operation. With a pair of varactors embedded into each radiating patch, the resonant frequencies of the lower and higher bands can be respectively tuned. Because the microstrip antenna is operated in its fundamental mode, broadside radiation patterns can be obtained at the two operation bands. The design in [2] adopts a suspended patch antenna with shorting posts. To achieve dual-frequency operation, four symmetrical resonant slots are cut on the patch. The feed point of the antenna is placed at the center of the patch so that monopolar modes can be excited. Consequently, conical radiation patterns are generated at the two operation bands; besides, the lower and higher operation frequencies can be respectively controlled with two independent voltages. Another design is based on a center-shortened microstrip patch antenna [3], and the fundamental mode and monopolar mode can be excited from the antenna structure at different frequencies. The antenna operated in the two bands can respectively radiate broadside and conical patterns; moreover, the operation frequencies can be tuned using two groups of varactors placed at the two opposite sides of the radiating patch. These dual-frequency reconfigurable antennas mentioned above only have one input port. However, an antenna with multiple feed ports may be required when it is applied to different communication systems.

In this paper, a dual-frequency antenna with three input ports is proposed. For the antenna, a slot mode and a monopolar-patch mode can be respectively excited at the lower and higher operation bands. In addition, the resonant frequency of the slot mode can be tuned using four varactors placed across the slot, and broadside radiations with dual orthogonal linear polarizations are obtained within

Received 12 March 2021, Accepted 14 April 2021, Scheduled 16 April 2021

* Corresponding author: Jeen-Sheen Row (jsrow@cc.ncue.edu.tw).

The authors are with the Department of Electrical Engineering, National Changhua University of Education, Chang-Hua 500, Taiwan, R.O.C.

the tunable band. As for the antenna operated in the monopolar-patch mode, the operation frequencies have less variations as the capacitance of the varactors is changed, and conical radiation patterns can be generated at a fixed band.

2. ANTENNA STRUCTURE

The structure of the proposed antenna is mainly composed of two FR4 printed circular boards with 0.8 mm thickness, as depicted in Fig. 1(c). A circular patch with a radius of 28 mm is printed on the bottom side of the upper FR4 substrate, and an annular slot with an inner radius of 19 mm and a slot width of 1 mm is embedded into the circular patch, as shown in Fig. 1(b). The slotted patch is placed above the lower FR4 substrate at a distance of 6 mm, and it is supported by four shorting posts of radius 1 mm. Two of the shorting posts are replaced with the outer conductors of 0.086 semi-rigid coaxial cables. The inner conductors of the two coaxial cables are extended to the top side of the upper FR4 substrate, and they are connected to dual orthogonal feed lines which are used to excite the annular slot. On the other hand, the slotted patch itself is also excited at its center with a probe feed, which is a standard SMA connector with an extended inner conductor, and consequently a monopolar-patch mode can also be excited. To reconfigure the resonant frequencies of the two modes, four varactors (SMV1232-079) are placed at the same layer as the feed lines, as shown in Fig. 1(a), and they are mounted across the annular slot with the aid of pads and via holes. The total size of the antenna, including a square ground plane, is $80 \times 80 \times 7.6 \text{ mm}^3$. Note that the operation of the proposed antenna is similar to that described in [12] where all of the input ports are excited at the same band for pattern diversity applications. Due to the presence of the varactors, the resonant frequencies of the slot mode and monopolar-patch mode are affected, and they would have different variations against capacitance value of the varactors. As a consequence, a dual-frequency reconfigurable antenna is created.

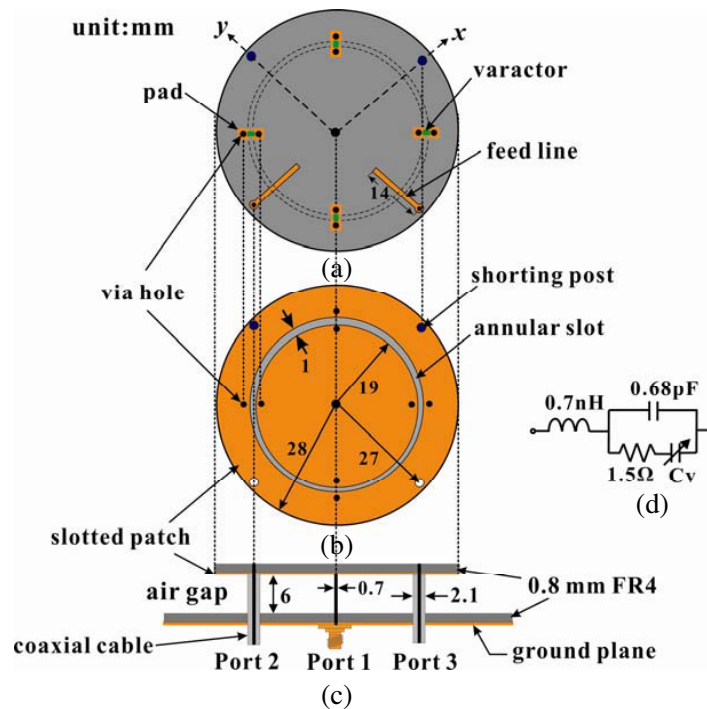


Figure 1. Geometry of the proposed antenna. (a) Layout of the top side of the upper FR4 substrate, (b) layout of the bottom side of the upper FR4 substrate, (c) side view of the antenna structure, (d) equivalent circuit of the used varactor.

3. SIMULATED AND MEASURED RESULTS

For the antenna with the parameters shown in Fig. 1, simulation analyses are performed with HFSS. In the simulation, each varactor is represented with its equivalent circuit given in Fig. 1(d). Figs. 2(a) and (b) present the return loss of the antenna respectively excited at Port 1 and Port 2. From the simulated results, it is found that the resonant frequency (f_m), defined as the frequency with minimum return loss, of the monopolar-patch mode is slightly decreased from 2.46 to 2.38 GHz as the capacitance C_V is increased from 0.6 to 1.8 pF; however, the resonant frequency (f_s) of the slot mode is considerably lowered from 1.62 to 1.17 GHz with an increase of C_V . The radiation patterns of the antenna operated in the monopolar-patch mode are exhibited in Fig. 3. Conical radiation is seen in the x - z and y - z planes, and the peak gain occurs around $\theta = \pm 50^\circ$. As for the slot mode, broadside patterns with linear polarization can be obtained within the tunable band. Typical results are plotted in Fig. 4 where the patterns at 1.2 GHz are presented in Figs. 4(a) and (b), and the patterns at 1.6 GHz are presented in Figs. 4(c) and (d). It has to be mentioned that because of symmetry, the return loss and radiation pattern of the antenna excited at Port 3 are the same as those at Port 2. The only difference between them is that the polarization directions are orthogonal to each other. The two orthogonal ports can be used to perform polarization diversity or generate a circular polarization radiation with a broadband 90° phase shifter feed network [13–15].

To validate the simulated results, a prototype of the proposed antenna is constructed, and its

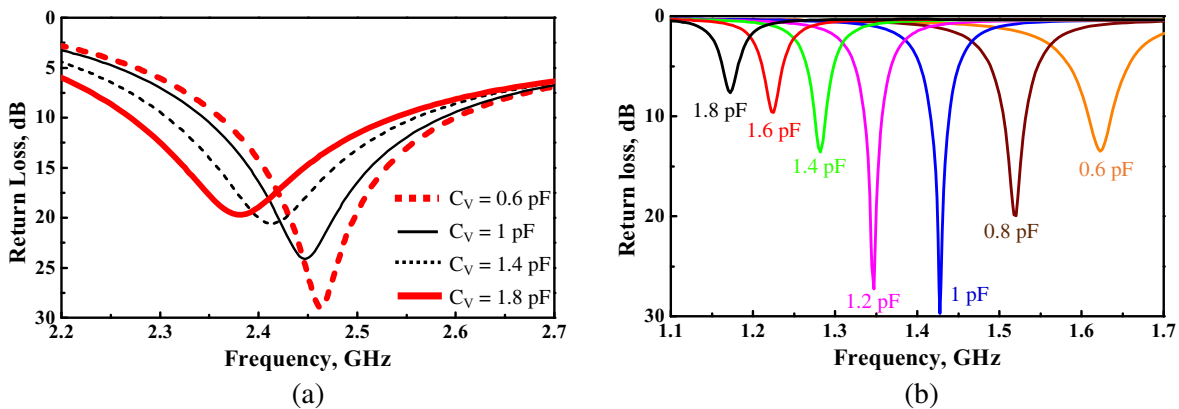


Figure 2. Simulated return loss of of the antenna excited at Port 1 and Port 2. (a) Port 1, (b) Port 2.

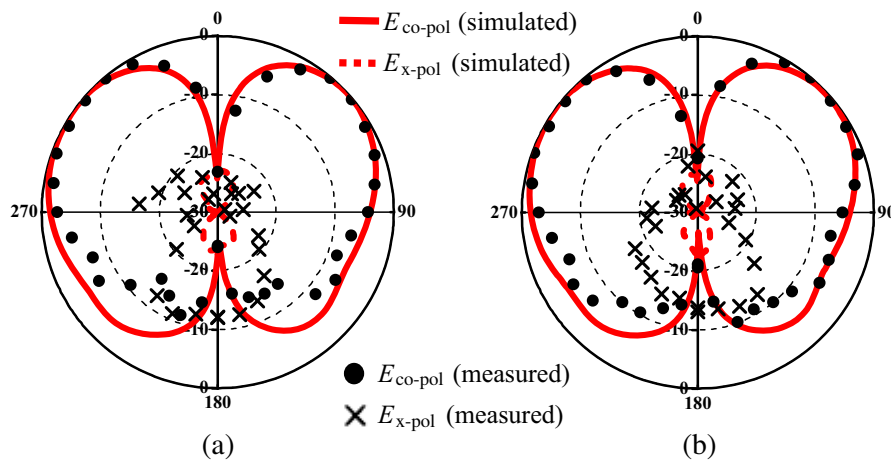


Figure 3. Radiation patterns of the antenna operated in monopolar-patch mode at 2.45 GHz. (a) x - z plane, (b) y - z plane.

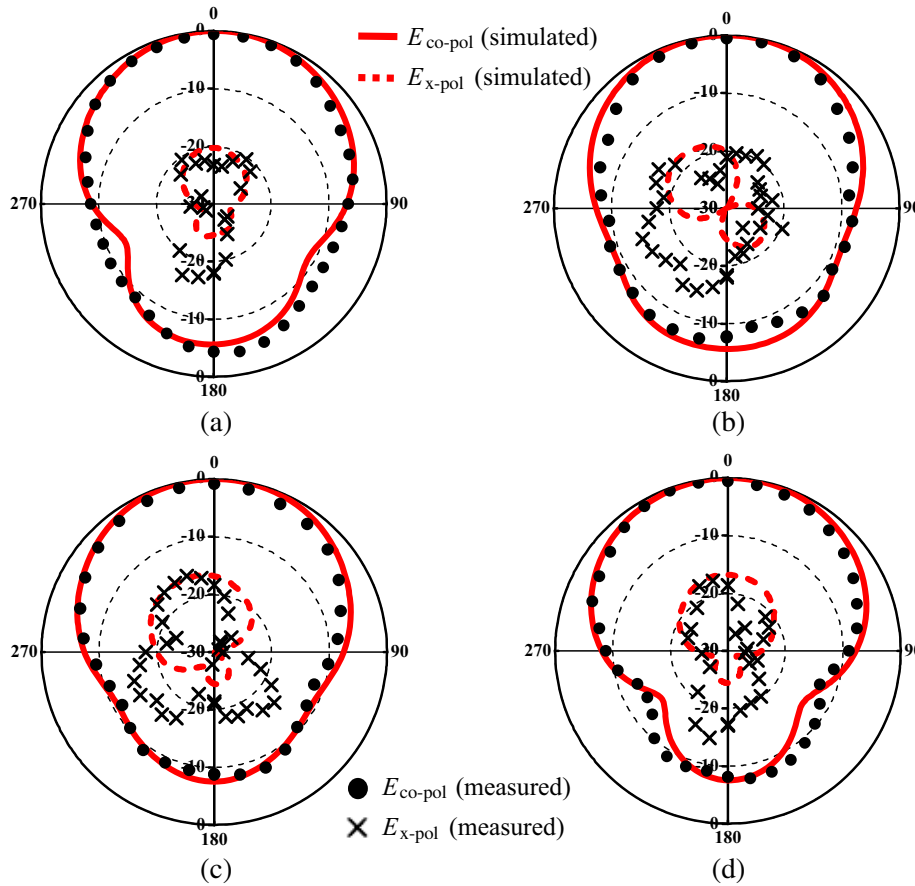


Figure 4. Radiation patterns of the antenna operated in slot mode at 1.2 GHz and 1.6 GHz. (a) x - z plane, 1.2 GHz, (b) y - z plane, 1.2 GHz, (c) x - z plane, 1.6 GHz, (d) y - z plane, 1.6 GHz.

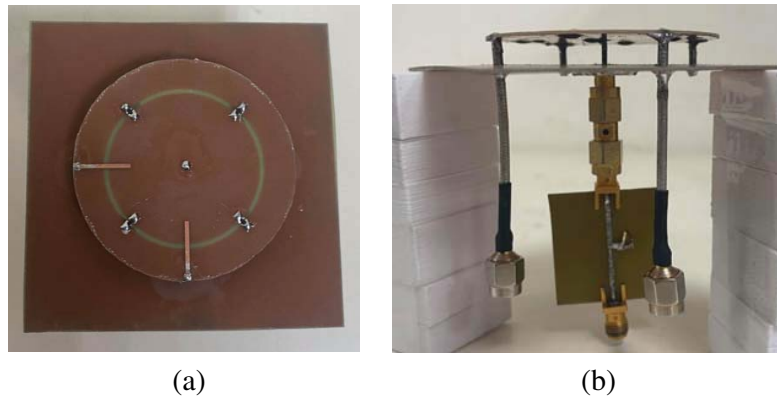


Figure 5. Photographs of the constructed prototype with a bias tee. (a) Top view, (b) side view.

photographs are exhibited in Fig. 5. A bias-tee, connected to Port 1, is required to control the dc voltage (V_R) of the varactors. For the cases of different V_R , the measured return loss of the prototype operating in the two modes is presented in Fig. 6. The results demonstrate that f_m and f_s respectively have the variations of 4% and 32% as V_R is increased from 2 to 12 V. Note that the tunable band of the slot mode can be moved to higher frequencies as long as a varactor with a lower C_V (< 0.6 pF) is used, and the impedance matching at the higher frequencies can be improved by shortening the length

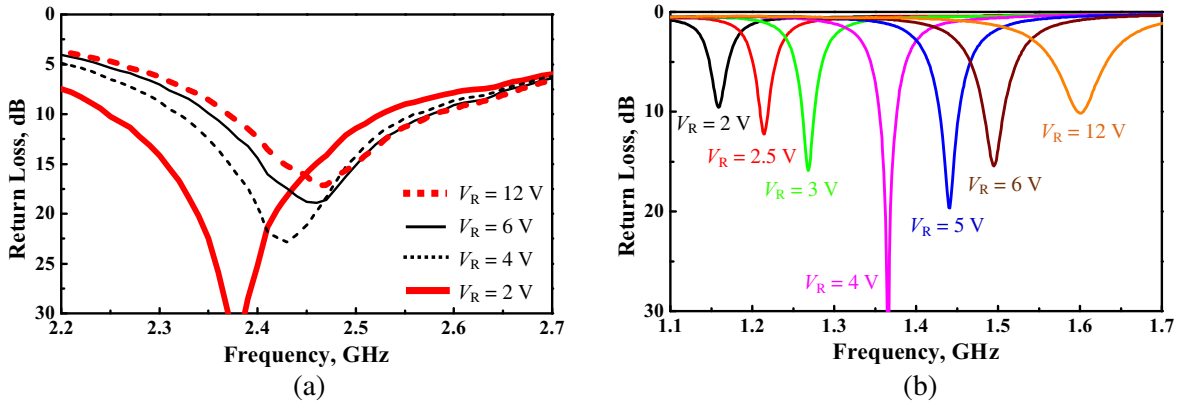


Figure 6. Measured return loss of of the antenna excited at Port 1 and Port 2. (a) Port 1, (b) Port 2.

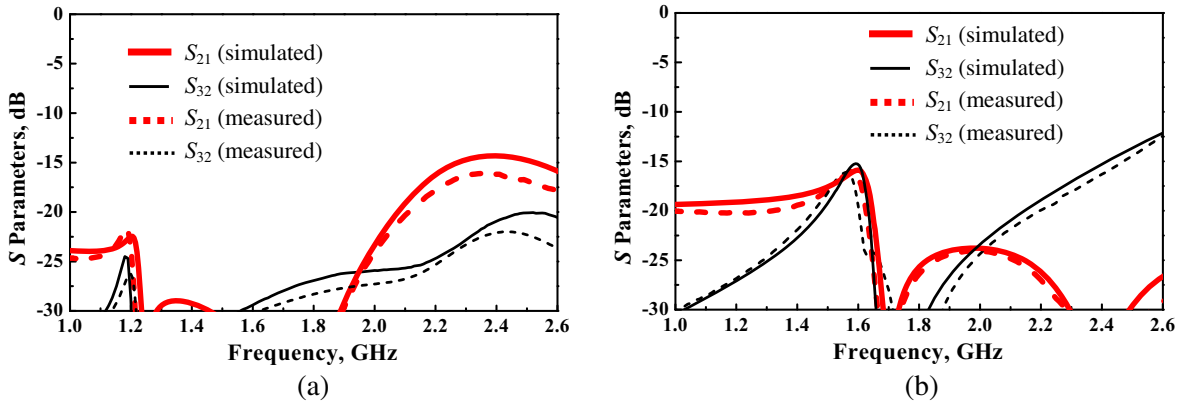


Figure 7. Measured (simulated) S parameters of the antenna. (a) $V_R = 2.5$ V ($C_V = 1.6$ pF), (b) $V_R = 12$ V ($C_V = 0.6$ pF).

of the feed lines. Because the effect of varying V_R on f_m is relatively little, the prototype operated in the monopolar-patch mode has a fixed 10 dB-return-loss impedance bandwidth, which is from 2.37 to 2.52 GHz, as V_R ranges between 2 and 12 V. The isolation levels between the input ports are also investigated, and the experimental results are exhibited in Fig. 7 along with the corresponding simulated data. For the case of $V_R = 2.5$ V, the measured isolation (S_{23}) between Ports 2 and 3 is about -25 dB at f_s , and the coupling (S_{21}) between Ports 1 and 2 at f_m is -15 dB. As V_R is changed to 12 V, S_{23} is increased to -15 dB at f_s , and S_{21} is decreased to -30 dB at f_m . For comparisons, the measured radiation patterns of the antenna operating at the two modes are respectively presented in Figs. 3 and 4. The peak gain of the conical pattern is almost constant as V_R is varied, and it is around 2.6 dBi at 2.45 GHz. However, the gain of the broadside pattern is degraded with decreasing f_s . The measured gain is 2 dBi at 1.6 GHz, and it is decreased to -1.7 dBi at 1.2 GHz. These gains can be improved by enlarging the size of the ground plane.

4. CONCLUSIONS

A frequency reconfigurable antenna with dual-band and dual-mode operation has been presented. Both measured and simulated results show that the antenna operated at the lower band can generate broadside radiation patterns with dual orthogonal linear polarizations, and the resonant frequency can be tuned between 1.2 and 1.6 GHz; in addition, the antenna operated at the higher band can generate conical radiation patterns, and a fixed impedance bandwidth around 2.45 GHz can also be obtained. The three radiation modes are excited with their corresponding input ports, and the isolation level between

any two ports is smaller than -15 dB when the frequency is tuned. For the two orthogonal linear polarization modes, they can be used to generate a circular polarization radiation as long as a hybrid coupler is introduced. The resultant broadside circularly polarized radiation will be applied to the Global Navigation Satellite System, and the conical radiation is suitable for terrestrial wireless communication systems.

REFERENCES

1. Ge, L., M. Li, J. Wang, and H. Gu, "Unidirectional dual-band stacked patch antenna with independent frequency reconfiguration," *IEEE Antennas Wireless Propag. Lett.*, Vol. 16, 113–116, 2017.
2. Nguyen-Trong, N., A. Piotrowski, and C. Fumeaux, "A frequency-reconfigurable dual-band low-profile monopolar antenna," *IEEE Trans. Antennas Propag.*, Vol. 65, 3336–3343, 2017.
3. Nguyen-Trong, N., L. Hall, and C. Fumeaux, "A frequency- and pattern-reconfigurable center-shortened microstrip antenna," *IEEE Antennas Wireless Propag. Lett.*, Vol. 15, 1955–1958, 2016.
4. Zhang, J., S. Yan, and G. A. E. Vandenbosch, "Radial CRLH-TL-based dual-band antenna with frequency agility," *IEEE Trans. Antennas Propag.*, Vol. 68, 5664–5669, 2020.
5. Al-Zayed, A. S., M. A. Kourah, and S. F. Mahmoud, "Frequency-reconfigurable single- and dual-band designs of a multi-mode microstrip antenna," *IET Microw. Antennas Propag.*, Vol. 8, 1105–1112, 2014.
6. Li, T., H. Zhai, X. Wang, L. Li, and C. Liang, "Frequency-reconfigurable bow-tie antenna for Bluetooth, WiMAX, and WLAN applications," *IEEE Antennas Wireless Propag. Lett.*, Vol. 14, 171–174, 2016.
7. Mayuri, P., N. D. Rani, N. B. Subrahmanyam, and B. T. Madhav, "Design and analysis of a compact reconfigurable dual band notched UWB antenna," *Progress In Electromagnetics Research C*, Vol. 98, 141–153, 2020.
8. Ge, L., Y. Li, J. Wang, and C. Y. D. Sim, "A low-profile reconfigurable cavity-backed slot antenna with frequency, polarization, and radiation pattern agility," *IEEE Trans. Antennas Propag.*, Vol. 65, 2182–2189, 2017.
9. Sharma, S. and C. C. Tripathi, "Frequency reconfigurable U-slot antenna for SDR application," *Progress In Electromagnetics Research Letters*, Vol. 55, 129–136, 2015.
10. Li, P. K., Z. H. Shao, Q. Wang, and Y. J. Cheng, "Frequency- and pattern reconfigurable antenna for multistandard wireless applications," *IEEE Antennas Wireless Propag. Lett.*, Vol. 14, 333–336, 2015.
11. Anu, A., P. Abdulla, P. M. Jasmine, and T. Rekha, "A varactor-tuned aperture coupled dual band cylindrical dielectric resonator antenna for C-band application," *Progress In Electromagnetics Research C*, Vol. 94, 261–272, 2019.
12. Row, J. S. and L. K. Kuo, "A pattern diversity antenna with six input ports," *Microwave and Opt. Technol. Lett.*, Vol. 62, 1252–1258, 2020.
13. Sun, C., H. Zheng, L. Zhang, and Y. Liu, "A compact frequency-reconfigurable patch antenna for Beidou (COMPASS) navigation system," *IEEE Antennas Wireless Propag. Lett.*, Vol. 13, 967–970, 2014.
14. Ferrero, F., C. Luxey, R. Staraj, G. Jacquemod, M. Yedlin, and V. Fusco, "Theory and design of a tunable quasi-lumped quadrature coupler," *Microwave and Opt. Technol. Lett.*, Vol. 51, 2219–2222, 2009.
15. Row, J. S. and C. J. Shih, "Polarization-diversity ring slot antenna with frequency agility," *IEEE Trans. Antennas Propag.*, Vol. 60, 3953–3957, 2012.